



Molybdenum(VI) tris(amidophenoxide) complexes

Journal:	<i>Dalton Transactions</i>
Manuscript ID	DT-ART-08-2018-003392.R1
Article Type:	Paper
Date Submitted by the Author:	14-Oct-2018
Complete List of Authors:	Erickson, Alexander; University of Notre Dame, Department of Chemistry and Biochemistry Brown, Seth; University of Notre Dame, Department of Chemistry and Biochemistry



Molybdenum(VI) tris(amidophenoxide) complexes

Alexander N. Erickson and Seth N. Brown^{*a}

Received 00th January 20xx,
Accepted 00th January 20xx

DOI: 10.1039/x0xx00000x

www.rsc.org/

Tris(2-(arylamido)-4,6-di-*tert*-butylphenoxy)molybdenum(VI) complexes (^Rap)₃Mo can be prepared either from (cycloheptatriene)Mo(CO)₃ and the *N*-aryliminoquinone, or from MoO₂(acac)₂ and the aminophenol. In contrast to all other reported unconstrained transition metal tris(amidophenoxide) complexes, the molybdenum complexes show a facial geometry in the solid state. In solution, the *fac* isomer predominates, though a small amount of *mer* isomer is detectable at room temperature. At elevated temperature the two species interconvert through Rây-Dutt trigonal twists, which are faster than Bailar twists in this system, presumably because of steric effects of the *N*-aryl groups. Substituents on the *N*-aryl ring shift the *fac/mer* equilibrium of the complex, with more electron-withdrawing substituents generally increasing the proportion of the *mer* isomer. The preference for *fac* over *mer* geometry is thus suggested to be due to enhanced π bonding in the *fac* isomer. In contrast to analogous catecholate complexes, the tris(amidophenoxide) complexes are not Lewis acidic and are inert to nucleophilic oxidants such as amine-*N*-oxides.

Introduction

Catecholate and the related amidophenoxide ligands, by virtue of their ease of oxidation, can confer redox activity on complexes of metal centers that would intrinsically be redox-inactive.¹ In particular, complexes of *d*⁰ metal centers such as molybdenum(VI) with such ligands can be oxidized by oxygen atom donors such as amine-*N*-oxides, where the metal center accepts the oxygen atom and the ligand donates the electrons, a process termed nonclassical oxygen atom transfer.² However, oxidation of molybdenum catecholates results in the release of free benzoquinones, which prevents applying the reaction to catalytic processes.^{3,4}

An established approach to stabilizing catecholate-type ancillary ligands toward dissociation in their (less Lewis basic) oxidized forms is to incorporate them as part of a larger polydentate ligand that can remain bound throughout a catalytic cycle.⁵ With this in mind, a tripodal tris(amidophenol) based on a tri-*p*-tolylamine core, tris(2-(3',5'-di-*tert*-butyl-2'-hydroxyphenyl)amino-4-methylphenyl)amine (MeClampH₆), was prepared.⁶ The ligand does confer good stability on its molybdenum(VI) complex, but the central amine donor binds to

molybdenum, quenching its Lewis acidity and rendering it unreactive towards oxidants.

Here we report the preparation and characterization of molybdenum tris(amidophenoxide) complexes containing simple bidentate 2-(arylamido)-4,6-di-*tert*-butylphenoxy (^Rap) ligands. Remarkably, the unconstrained six-coordinate complexes (^Rap)₃Mo share with the constrained seven-coordinate (MeClamp)Mo both a preference for the *fac* geometry and low Lewis acidity. The ease of variation of *para* substituents on the *N*-aryl group allows one to vary the electronic properties of the ligands, which sheds light on the bonding in these complexes.

Experimental Section

General procedures

Unless otherwise noted, all procedures were carried out under an inert atmosphere in a nitrogen-filled glovebox or on a vacuum line. When dry solvents were needed, they were purchased from Acros Organics and stored in the glovebox. Deuterated solvents were obtained from Cambridge Isotope Laboratories, dried as described, and stored in the drybox prior to use. CD₂Cl₂, CDCl₃, and CD₃CN were dried over 4 Å molecular sieves, followed by CaH₂. C₆D₆ and C₆D₅CD₃ were dried over sodium, and tetrahydrofuran-*d*₈ over sodium benzophenone ketyl. All other reagents were commercially available and used without further purification. Unless otherwise noted, routine NMR spectra were taken between 22 °C and 25 °C and were measured on a Bruker Avance DPX 400 spectrometer. Variable-temperature NMR spectra were measured on this instrument or on a Varian Inova

^a Department of Chemistry and Biochemistry, 251 Nieuwland Science Hall, University of Notre Dame, Notre Dame, IN 46556-5670, USA. Fax: 01 574 631 6652; Tel: 01 574 631 4659; E-mail: Seth.N.Brown.114@nd.edu

Electronic Supplementary Information (ESI) available: CCDC deposition numbers 1862122-1862128; additional crystallographic, spectroscopic, electrochemical, and computational details. See DOI: 10.1039/x0xx00000x

500 spectrometer, with temperatures calibrated using the chemical shifts in methanol or ethylene glycol.⁷ Chemical shifts for ¹H and ¹³C{¹H} spectra are reported in ppm downfield of TMS, with spectra referenced using the known chemical shifts of the solvent residuals. For the (ap)₃Mo compounds, only resonances due to the major (*fac*) isomers are reported. ¹⁹F spectra are reported in ppm downfield of CFCl₃ as an internal standard. Infrared spectra were recorded on a Jasco 6300 FT-IR spectrometer as powders on ATR plates. UV-Visible spectra were recorded in 1-cm quartz cells on a ThermoFisher Evolution Array spectrophotometer. Elemental analyses were performed by M-H-W Laboratories (Phoenix, AZ).

Syntheses

2-Phenylimino-4,6-di-*tert*-butyl-1,2-benzoquinone, ^{hiq}. To a 50 mL round-bottom flask were added 0.4133 g 2-phenylamino-4,6-di-*tert*-butylphenol (^{hap}H₂)⁸ (1.39 mmol) and 0.4480 g iodobenzene diacetate (1.39 mmol). A stir bar was added and the solids were dissolved in 10 mL CHCl₃. Immediately upon mixing, the solution changed color to dark red-orange. The reaction was stirred for 10 min and the solvent evaporated on the vacuum line. The oily residue was dissolved in a minimum of pentane and left in the freezer to crystallize. After 2 d at -30 °C, the solid was filtered and dried, furnishing 0.2021 g ^{hiq} (49%) as a mixture of *E* and *Z* isomers (97:3 by ¹H NMR integration). ¹H NMR (CDCl₃): *E* isomer δ 7.36 (t, 7.5 Hz, 2H, *m*-Ph), 7.17 (t, 7.5 Hz, 1H, *p*-Ph), 7.02 (d, 2.3 Hz, 1H, *iq* H-3 or -5), 6.91 (d, 7.5 Hz, 2H, *o*-Ph), 6.30 (d, 2.3 Hz, 1H, *iq* H-3 or -5), 1.32 (s, 9H, ^tBu), 1.12 (s, 9H, ^tBu). *Z* isomer δ 7.31 (t, 8.3 Hz, 2H, *m*-Ph), 7.08 (t, 7.5 Hz, 1H, *p*-Ph), 6.72 (d, 8.4 Hz, 2H, *o*-Ph), 6.48 (d, 2.5 Hz, 1H, *iq* H-3 or -5) 1.24 (s, 9H, ^tBu), 1.19 (s, 9H, ^tBu) [one aromatic resonance obscured by *E* isomer]. ¹³C{¹H} NMR (CDCl₃, *E* isomer only): δ 184.25 (C=O), 156.64, 153.79, 150.28, 149.02, 133.99, 128.90, 125.56, 120.68, 114.50, 35.65 (C(CH₃)₃), 35.55 (C(CH₃)₃), 29.57 (C(CH₃)₃), 28.63 (C(CH₃)₃). IR (cm⁻¹): 3063 (w), 3001 (w), 2958 (m), 2868 (w), 1660 (s, ν_{C=O}), 1625 (m), 1590 (w), 1573 (w), 1540 (w), 1479 (m), 1464 (m), 1388 (w), 1371 (s), 1323 (w), 1272 (m), 1247 (m), 1213 (m), 1170 (w), 1084 (w), 1072 (m), 1023 (m), 988 (w), 968 (m), 928 (w), 911 (w), 896 (s), 873 (s), 834 (m), 804 (s), 792 (m), 759 (s), 736 (m), 697 (s). UV-Vis (CH₂Cl₂): λ_{max} = 290 nm (ε = 4200 L mol⁻¹ cm⁻¹), 405 (4900), 488 (sh, 3400). Anal. Calcd for C₂₀H₂₅NO: C, 81.31; H, 8.53; N, 4.74. Found: C, 81.62; H, 8.40; N, 4.08.

Tris(2-phenylamido-4,6-di-*tert*-butylphenoxo)molybdenum(VI), (^{hap})₃Mo. To generate 2-phenylimino-4,6-di-*tert*-butyl-1,2-benzoquinone, 0.3045 g ^{hap}H₂ (1.024 mmol) and 0.3297 g PhI(OAc)₂ (1.023 mmol) were reacted in CHCl₃ as described above and the solvent evaporated on the vacuum line. To the crude residue was added a solution of 0.0932 g cycloheptatrienemolybdenum tricarbonyl (0.342 mmol, 0.33 eq) in 12 mL C₆H₆. After stirring 24 h at room temperature, the solvent was pumped off. The residue was slurried with 2 mL CH₃CN and the liquid decanted away from the undissolved solid.

The solid was collected and dried under vacuum for 1 h to give 0.2020 g (^{hap})₃Mo (59%). ¹H NMR (CDCl₃): δ 7.09 (t, 7.9 Hz, 3H, *p*-Ph), 6.98 (t, 7.8 Hz, 6H, *m*-Ph), 6.92 (d, 1.9 Hz, 3H, *ap* H-3 or -5), 5.78 (d, 1.9 Hz, 3H, *ap* H-3 or -5), 5.31 (v br s, 6H, *o*-Ph), 1.48 (s, 27H, ^tBu), 1.11 (s, 27H, ^tBu). ¹H NMR (CD₂Cl₂, -70.5 °C): δ 7.11 (t, 7.2 Hz, 3H, *p*-Ph), 7.01 (t, 7.5 Hz, 3H, *m*-Ph), 6.90 (t, 7.5 Hz, 3H, *m*-Ph), 6.90 (s, 3H, *ap* H-3 or -5), 5.83 (s, 3H, *ap* H-3 or -5), 5.80 (d, 7.8 Hz, 3H, *o*-Ph), 4.17 (d, 7.8 Hz, 3H, *o*-Ph), 1.44 (s, 27H, ^tBu), 1.06 (s, 27H, ^tBu). ¹³C{¹H} NMR (CD₂Cl₂, -70.5 °C) δ 160.19 (OC), 151.28, 149.46, 141.16, 134.87, 128.11, 127.06, 126.75, 126.31, 124.23, 122.43, 108.99, 34.72 (C(CH₃)₃), 34.00 (C(CH₃)₃), 31.11 (C(CH₃)₃), 28.61 (C(CH₃)₃). IR (cm⁻¹): 3374 (w), 3059 (w), 2951 (s), 2866 (m), 2702 (w), 1982 (w), 1762 (w), 1588 (m), 1550 (m), 1477 (s), 1438 (m), 1420 (m), 1391 (m), 1360 (m), 1294 (w), 1277 (m), 1243 (s), 1231 (s), 1200 (s), 1161 (s), 1118 (w), 1072 (w), 1025 (m), 989 (w), 926 (w), 915 (w), 881 (w), 861 (m), 832 (m), 765 (m), 742 (m), 731 (m), 701 (s), 677 (m). UV-Vis (CH₂Cl₂): λ_{max} = 288 nm (ε = 28200 L mol⁻¹ cm⁻¹), 389 (13900), 482 (33200), 650 (13500), 803 (9300). Anal. Calcd for C₆₀H₇₅MoN₃O₃: C, 73.37; H, 7.70; N, 4.28. Found: C, 73.81; H, 7.57; N, 3.91.

2-(4-Benzylphenyl)amino-4,6-di-*tert*-butylphenol, (^{PhCH₂ap}H₂). To a 25 mL Erlenmeyer flask in the air was added 0.9042 g 4-benzylaniline (4.93 mmol) and 1.0977 g 3,5-di-*tert*-butylcatechol (4.94 mmol). Hexanes (7 mL) were added, and after stirring the mixture briefly, 52 μL Et₃N (0.37 mmol, 0.075 eq) was added. Upon addition of the Et₃N, the solution changed to a dark brown color. The flask was sealed with parafilm and allowed to stir overnight. The solution was vacuum filtered through a glass frit and the solid washed with 2 × 5 mL cold hexanes. After air drying for an hour, the yield of 2-(4-benzylphenyl)amino-4,6-di-*tert*-butylphenol was 1.4672 g (76%). ¹H NMR (C₆D₆) δ 7.43 (d, 2.2 Hz, 1H, *ap* H-3 or -5), 7.11 (t, 2H, 8 Hz, *m*-C₆H₅CH₂), 7.06 (d, 7.0 Hz, 2H, *o*-C₆H₅CH₂), 7.02 (t, 7.0 Hz, 1H, *p*-C₆H₅CH₂), 6.96 (d, 2.2 Hz, 1H, *ap* H-3 or -5), 6.88 (d, 8.3 Hz, 2H, *m*-NHC₆H₄Bn), 6.42 (d, 8.3 Hz, 2H, *o*-NHC₆H₄Bn), 6.37 (s, 1H, OH), 4.02 (s, 1H, NH), 3.69 (s, 2H, CH₂), 1.63 (s, 9H, ^tBu), 1.24 (s, 9H, ^tBu). ¹³C{¹H} NMR (C₆D₆) δ 150.44 (HOC), 145.72, 142.67, 142.43, 135.87, 133.20, 130.46, 129.56, 129.18, 129.01, 126.54, 122.35, 115.94, 41.75 (CH₂), 35.69 (C(CH₃)₃), 34.84 (C(CH₃)₃), 32.14 (C(CH₃)₃), 30.19 (C(CH₃)₃). IR (cm⁻¹): 3452 (m, ν_{OH}), 3354 (m, ν_{NH}), 2958 (m), 2883 (m), 1954 (w), 1890 (w), 1769 (w), 1612 (m), 1510 (s), 1482 (m), 1453 (m), 1443 (m), 1416 (m), 1389 (w), 1359 (m), 1312 (s), 1267 (w), 1236 (m), 1218 (s), 1199 (s), 1174 (m), 1154 (m), 1116 (m), 1073 (m), 1026 (m), 973 (m), 912 (w), 903 (w), 880 (m), 856 (w), 833 (m), 819 (m), 806 (m), 794 (m), 760 (s), 734 (m), 700 (s). Anal. Calcd for C₂₇H₃₃NO: C, 83.68; H, 8.58; N, 3.61. Found: C, 83.47; H, 8.63; N, 3.54.

Tris(2-(4-benzylphenyl)amido-4,6-di-*tert*-butylphenoxo)molybdenum(VI), (^{PhCH₂ap})₃Mo. To a 20 mL scintillation vial was added 0.0610 g MoO₂(acac)₂ (0.187 mmol) and a stirbar. A solution of 0.2174 g ^{PhCH₂ap}H₂ (0.561 mmol, 3.00 equiv) in 8 mL toluene was added to the vial, which was then capped and taken out of the drybox. After being heated for 5 d in a 110 °C oil bath,

with stirring, the solution was transferred to a round-bottom flask in the glovebox. The solvent was evaporated on the vacuum line and the oily residue dissolved in 2 mL toluene. After the solution was allowed to stand at $-30\text{ }^{\circ}\text{C}$ for 2 weeks, the crystals were collected via filtration and dried to give 0.1386 g ($^{\text{PhCH}_2\text{ap}}_3\text{Mo}$) (59%). ^1H NMR (toluene- d_8 , $-70.5\text{ }^{\circ}\text{C}$): δ 7.29 (t, 7.4 Hz, 3H, *p*- $\text{C}_6\text{H}_5\text{CH}_2$), 7.15 (m, 12H, *o*- and *m*- $\text{C}_6\text{H}_5\text{CH}_2$), 7.00 (s, 3H, *ap* H-3 or -5), 6.83 (d, 8.0 Hz, 3H, *m*- $\text{NC}_6\text{H}_4\text{Bn}$), 6.37 (d, 8.0 Hz, 3H, *o*- $\text{NC}_6\text{H}_4\text{Bn}$), 6.19 (s, 3H, *ap* H-3 or -5), 6.09 (d, 7.8 Hz, 3H, *m*- $\text{NC}_6\text{H}_4\text{Bn}$), 4.16 (d, 7.8 Hz, 3H, *o*- $\text{NC}_6\text{H}_4\text{Bn}$), 3.53 (d, 13.8 Hz, 3H, *CHH'*), 3.40 (d, 13.8 Hz, 3H, *CHH'*), 1.77 (s, 27H, ^tBu), 1.10 (s, 27H, ^tBu). IR (cm^{-1}): 3210 (w), 3063 (w), 3023 (w), 2950 (s), 2865 (m), 1600 (w), 1582 (w), 1552 (m), 1500 (m), 1476 (m), 1454 (m), 1440 (m), 1413 (w), 1390 (w), 1360 (m), 1301 (m), 1279 (m), 1250 (s), 1200 (m), 1178 (w), 1161 (s), 1107 (w), 1072 (w), 1029 (w), 1017 (m), 988 (m), 950 (w), 919 (m), 899 (w), 879 (w), 860 (m), 834 (m), 790 (m), 769 (m), 755 (m), 728 (s), 720 (s), 695 (s), 674 (m). UV-Vis (CH_2Cl_2): $\lambda_{\text{max}} = 322\text{ nm}$ (sh, $\epsilon = 13500\text{ L mol}^{-1}\text{ cm}^{-1}$), 390 (10700), 481 (22200), 656 (8100), 816 (7800). Anal. Calcd for $\text{C}_{81}\text{H}_{93}\text{MoN}_3\text{O}_3$: C, 77.67; H, 7.48; N, 3.35. Found: C, 77.55; H, 7.33; N, 3.11.

2-(4-Trifluoromethylphenyl)imino-4,6-di-*tert*-butyl-1,2-benzoquinone, $^{\text{CF}_3\text{iq}}$. To a 50 mL round bottom flask was added 0.2233 g 2-(4-trifluoromethylphenyl)amino-4,6-di-*tert*-butylphenol⁹ (0.611 mmol) and 0.1973 g iodobenzene diacetate (0.612 mmol). A stir bar was added and the solids were dissolved in 10 mL CHCl_3 . The dark red-orange reaction mixture was stirred overnight and the chloroform was removed on the vacuum line. The residue was dissolved in a minimum of pentane and allowed to crystallize over 14 d at $-30\text{ }^{\circ}\text{C}$ to furnish, after filtration and drying under vacuum, 0.1832 g $^{\text{CF}_3\text{iq}}$ (82%) as a 95:5 mixture of *E* and *Z* isomers. ^1H NMR (CDCl_3), *E* isomer: δ 7.62 (d, 8.2 Hz, 2H, *m*- $\text{NC}_6\text{H}_4\text{CF}_3$), 7.02 (d, 2.0 Hz, 1H, *iq* H-3 or -5), 6.96 (d, 8.2 Hz, 2H, *o*- $\text{NC}_6\text{H}_4\text{CF}_3$), 6.14 (d, 2.0 Hz, 1H, *iq* H-3 or -5), 1.32 (s, 9H, ^tBu), 1.12 (s, 9H, ^tBu). *Z* isomer: δ 7.56 (d, 8.3 Hz, 2H, *m*- $\text{NC}_6\text{H}_4\text{CF}_3$), 6.73 (d, 8.3 Hz, 2H, *o*- $\text{NC}_6\text{H}_4\text{CF}_3$), 6.49 (d, 2.2 Hz, 1H, *iq* H-3 or -5), 1.25 (s, 9H, ^tBu), 1.18 (s, 9H, ^tBu) [one aromatic resonance obscured by *E* isomer]. $^{13}\text{C}\{^1\text{H}\}$ NMR (CDCl_3 , *E* isomer only): δ 183.88 (C=O), 156.99, 155.52, 153.38, 149.27, 134.04, 127.20 (q, $^2J_{\text{CF}} = 33\text{ Hz}$), 126.26 (q, $^3J_{\text{CF}} = 3.8\text{ Hz}$), 124.45 (q, $^1J_{\text{CF}} = 271\text{ Hz}$, CF_3), 120.09, 114.02, 35.86 ($\text{C}(\text{CH}_3)_3$), 35.60 ($\text{C}(\text{CH}_3)_3$), 29.54 ($\text{C}(\text{CH}_3)_3$), 28.54 ($\text{C}(\text{CH}_3)_3$). ^{19}F NMR (CDCl_3): δ -62.55 (*E* isomer), -62.20 (*Z* isomer). IR (cm^{-1}): 3066 (w), 2966 (m), 2873 (w), 1663 (s, $\nu_{\text{C=O}}$), 1622 (m), 1607 (m), 1572 (w), 1546 (m), 1505 (w), 1482 (w), 1467 (w), 1455 (w), 1413 (w), 1388 (w), 1366 (m), 1356 (w), 1320 (s), 1274 (m), 1246 (m), 1218 (m), 1179 (w), 1156 (s), 1120 (s), 1105 (s), 1065 (s), 1022 (w), 1011 (m), 981 (w), 967 (w), 929 (w), 914 (w), 894 (m), 875 (m), 860 (s), 835 (m), 802 (m), 785 (w), 764 (w), 733 (m), 684 (m). UV-Vis (CH_2Cl_2): $\lambda_{\text{max}} = 285\text{ nm}$ ($\epsilon = 5100\text{ L mol}^{-1}\text{ cm}^{-1}$), 409 (5500), 497 (2400). Anal. Calcd for $\text{C}_{21}\text{H}_{24}\text{F}_3\text{NO}$: C, 69.40; H, 6.66; N, 3.85. Found: C, 69.51; H, 6.49; N, 3.64.

Tris(2-(4-trifluoromethylphenyl)amido-4,6-di-*tert*-butylphenoxo)molybdenum(VI), ($^{\text{CF}_3\text{ap}}_3\text{Mo}$). The iminoquinone was generated by stirring a solution of 0.2068 g $^{\text{CF}_3\text{apH}_2}$ (0.566 mmol) and 0.1833 g $\text{Ph}(\text{OAc})_2$ (0.569 mmol) in 7 mL CHCl_3 for 24 h at room temperature. After removal of the solvent, the residue was treated with a solution of 0.0523 g cycloheptatrienemolybdenum tricarbonyl (0.192 mmol, 0.34 equiv) in 10 mL C_6H_6 . After 24 h at room temperature, the benzene was removed in vacuo. The oily residue was dissolved in a minimal amount of CH_3CN ($\sim 5\text{ mL}$) and crystallized over 7 d at $-30\text{ }^{\circ}\text{C}$. The solid was filtered and dried under vacuum, yielding 0.1853 g ($^{\text{CF}_3\text{ap}}_3\text{Mo}$) (83%). ^1H NMR (toluene- d_8): δ 7.45 (d, 7.7 Hz, 6H, *m*- $\text{NC}_6\text{H}_4\text{CF}_3$), 6.82 (s, 3H, *ap* H-3 or -5), 5.99 (s, 3H, *ap* H-3 or -5), 5.69 (br s, 6H, *o*- $\text{NC}_6\text{H}_4\text{CF}_3$), 1.63 (s, 27H, ^tBu), 1.02 (s, 27H, ^tBu). ^{19}F NMR (toluene- d_8): δ -62.17 . IR (cm^{-1}): 3076 (w), 2953 (m), 2907 (m), 2869 (m), 1917 (w), 1770 (w), 1609 (m), 1582 (w), 1552 (m), 1507 (m), 1479 (m), 1456 (m), 1440 (m), 1409 (m), 1394 (m), 1361 (m), 1321 (s), 1298 (s), 1280 (m), 1250 (s), 1232 (m), 1201 (m), 1163 (s), 1123 (s), 1105 (s), 1066 (s), 1026 (m), 1016 (s), 990 (m), 954 (m), 918 (m), 897 (m), 886 (m), 859 (m), 846 (s), 831 (m), 815 (s), 777 (m), 768 (s), 745 (m), 721 (m), 697 (s), 656 (m). UV-vis (CH_2Cl_2): $\lambda_{\text{max}} = 291\text{ nm}$ ($\epsilon = 23800\text{ L mol}^{-1}\text{ cm}^{-1}$), 400 (10800), 496 (27700), 678 (10000), 837 (7900). Anal. Calcd for $\text{C}_{63}\text{H}_{72}\text{F}_9\text{MoN}_3\text{O}_3$: C, 63.79; H, 6.12; N, 3.54. Found: C, 63.88; H, 6.03; N, 3.45.

Tris(2-(4-methoxyphenyl)amido-4,6-di-*tert*-butylphenoxo)molybdenum(VI), ($^{\text{CH}_3\text{Oap}}_3\text{Mo}$). The compound was prepared analogously to ($^{\text{PhCH}_2\text{ap}}_3\text{Mo}$) by heating 0.1155 g $\text{MoO}_2(\text{acac})_2$ (0.345 mmol) and 0.3483 g $^{\text{MeOapH}_2}$ ¹⁰ (1.063 mmol, 3.0 equiv) in 7 mL toluene in a $110\text{ }^{\circ}\text{C}$ oil bath for 4 d. Evaporation of the solvent and crystallization of the residue from 3 mL CH_3CN furnished 0.2932 g ($^{\text{MeOap}}_3\text{Mo}$) (77%). ^1H NMR (toluene- d_8): δ 7.13 (d, 1.9 Hz, 3H, *ap* H-3 or -5), 6.64 (d, 8.8 Hz, 6H, *m*- $\text{NC}_6\text{H}_4\text{OMe}$), 6.22 (d, 1.9 Hz, 3H, *ap* H-3 or -5), 5.78 (br s, 6H, *o*- $\text{NC}_6\text{H}_4\text{OMe}$), 3.28 (s, 9H, OCH_3), 1.70 (s, 27H, ^tBu), 1.11 (s, 27H, ^tBu). IR (cm^{-1}): 2952 (s), 2903 (s), 2866 (m), 1759 (w), 1718 (w), 1594 (m), 1581 (m), 1552 (m), 1476 (m), 1464 (m), 1440 (m), 1421 (m), 1392 (m), 1361 (s), 1301 (m), 1280 (m), 1240 (m), 1221 (m), 1200 (m), 1180 (s), 1120 (w), 1084 (w), 1035 (w), 1025 (w), 1003 (m), 957 (w), 933 (w), 915 (m), 899 (w), 879 (m), 862 (m), 841 (w), 823 (w), 770 (m), 761 (m), 730 (m), 709 (m), 660 (w). UV-vis (CH_2Cl_2): $\lambda_{\text{max}} = 281\text{ nm}$ ($\epsilon = 28700\text{ L mol}^{-1}\text{ cm}^{-1}$), 320 (15000), 393 (14200), 481 (31000), 648 (12200), 801 (8600). Anal. Calcd for $\text{C}_{63}\text{H}_{81}\text{MoN}_3\text{O}_6$: C, 70.57; H, 7.61; N, 3.92. Found: C, 70.75; H, 7.47; N, 3.91.

Tris(2-(3,5-di-*tert*-butylphenyl)amido-4,6-di-*tert*-butylphenoxo)molybdenum(VI), ($^{\text{tBu}_2\text{ap}}_3\text{Mo}$). The compound was prepared analogously to ($^{\text{Hap}}_3\text{Mo}$) by initially reacting 0.2150 g (0.525 mmol) 2-(3,5-di-*tert*-butylphenyl)amino-4,6-di-*tert*-butylphenol ($^{\text{tBu}_2\text{apH}_2}$)¹¹ and 0.1716 g (0.533 mmol, 1.02 equiv) iodobenzene diacetate in 10 mL CHCl_3 for 15 min at room temperature. The dark residue of $^{\text{tBu}_2\text{iq}}$ formed after evaporation of the solvent on the vacuum line was not isolated

but was characterized by ^1H NMR (CDCl_3): δ 7.23 (s, 1H, *p*- $\text{C}_6\text{H}_3^t\text{Bu}_2$), 7.03 (s, 1H, *iq* H-3 or -5), 6.84 (s, 2H, *o*- $\text{C}_6\text{H}_3^t\text{Bu}_2$), 6.46 (s, 1H, *iq* H-3 or -5), 1.33 (s, 9H, *iq*- ^tBu), 1.32 (s, 18H, Ar- ^tBu), 1.14 (s, 9H, *iq*- ^tBu).

The crude $^{t\text{Bu}_2\text{iq}}$ was mixed in the drybox with 0.0483 g (0.177 mmol, 0.34 equiv) cycloheptatrienemolybdenum tricarbonyl and 10 mL C_6H_6 . After stirring 24 h at room temperature the solvent was removed *in vacuo* and the residue dissolved in CHCl_3 and layered with CH_3CN . After 7 d the solid was collected and dried, furnishing 0.1873 g ($^{t\text{Bu}_2\text{ap}}_3\text{Mo}$) (80%). ^1H NMR (toluene- d_8): δ 7.35 (s, 3H, *p*- $\text{C}_6\text{H}_3^t\text{Bu}_2$), 6.98 (sl br s, 3H, *o*- $\text{C}_6\text{H}_3^t\text{Bu}_2$), 6.95 (d, 1.4 Hz, 3H, *ap* H-3 or -5), 5.96 (d, 1.4 Hz, 3H, *ap* H-3 or -5), 5.60 (sl br s, 3H, *o*- $\text{C}_6\text{H}_3^t\text{Bu}_2$), 1.67 (s, 27H, *ap* ^tBu), 1.19 (sl br s, 27H, Ar ^tBu), 1.10 (sl br s, 27H, Ar ^tBu), 0.99 (s, 27H, *ap* ^tBu). IR (cm^{-1}): 3075 (w), 2952 (s), 2903 (m), 2866 (m), 1759 (w), 1718 (w), 1594 (m), 1581 (m), 1552 (m), 1476 (m), 1464 (m), 1440 (m), 1421 (m), 1392 (m), 1381 (s), 1301 (m), 1280 (m), 1248 (m), 1221 (m), 1200 (m), 1160 (s), 1120 (w), 1084 (w), 1035 (m), 1025 (m), 1003 (s), 957 (w), 933 (w), 915 (w), 899 (w), 879 (m), 862 (m), 841 (w), 823 (m), 770 (s), 720 (s), 709 (m), 660 (w). UV-vis (CH_2Cl_2): λ_{max} = 296 nm (ϵ = 17700 L mol $^{-1}$ cm $^{-1}$), 333 (13100), 476 (28800), 693 (10500), 850 (7000). Anal. Calcd for $\text{C}_{84}\text{H}_{123}\text{MoN}_3\text{O}_3$: C, 76.50; H, 9.40; N, 3.19. Found: C, 76.55; H, 9.51; N, 3.02.

Electrochemistry

Cyclic voltammetry was performed at a scan rate of 60 mV s $^{-1}$ using an Autolab potentiostat (PGSTAT 128N), with glassy carbon working and counter electrodes and a silver/silver chloride reference electrode. The electrodes were connected to the potentiostat through electrical conduits in the drybox faceplate. Samples were approximately 1 mM in CH_2Cl_2 with 0.1 M Bu_4NPF_6 as the electrolyte. Potentials for the metal complexes were referenced to ferrocene/ferrocenium at 0 V with the reference potential established by spiking the test solution with a small amount of ferrocene. Potentials for the iminoquinones were

referenced to ferrocene with the reference potential established by spiking the test solution with a small amount of dexamethylferrocene (E° = -0.565 V vs. $\text{Cp}_2\text{Fe}^+/\text{Cp}_2\text{Fe}$).¹²

X-ray crystallography

Crystals were placed in inert oil before transferring to the N_2 cold stream of a Bruker Apex II CCD diffractometer. Data were reduced, correcting for absorption, using the program SADABS. The structures were solved using direct methods. All nonhydrogen atoms not apparent from the initial solutions were found on difference Fourier maps, and all heavy atoms were refined anisotropically. When disorder of *tert*-butyl groups in two orientations was observed, it was modeled by constraining the thermal parameters of opposing methyl carbons to be equal and refining the occupancy of each orientation. In ($^{\text{MeOap}}_3\text{Mo}$) \cdot 0.67 CH_3CN , one of the acetonitrile molecules (containing N11) was modeled in three orientations while restraining the C-N (1.16) and C-C (1.46) bond distances. In ($^{t\text{Bu}_2\text{ap}}_3\text{Mo}$) \cdot CDCl_3 \cdot 2.5 CH_3CN , the chloroform molecule was modeled in two orientations offset by about 20 $^\circ$, with the major component refining to 80.1(4)% occupancy. The acetonitrile molecule containing N93 was only partially occupied, and its occupancy was fixed arbitrarily at 0.5. In ($^{\text{CF}_3\text{ap}}_3\text{Mo}$) \cdot 2.5 CHCl_3 \cdot CH_3CN , one of the lattice chloroform molecules was disordered about the inversion center; the C-Cl bond distances in this molecule were fixed at 1.74 Å. In ($^{\text{MeOap}}_3\text{Mo}$) \cdot 0.67 CH_3CN and ($^{\text{CF}_3\text{ap}}_3\text{Mo}$) \cdot 2.5 CHCl_3 \cdot CH_3CN , all hydrogens were placed in calculated positions. In the other structures, hydrogens were found on difference Fourier maps and refined isotropically, except for the hydrogens on disordered *tert*-butyl groups and those on the lattice acetonitriles in ($^{t\text{Bu}_2\text{ap}}_3\text{Mo}$) \cdot CDCl_3 \cdot 2.5 CH_3CN . Hydrogen atoms that were placed in calculated positions had their thermal parameters tied to the isotropic thermal parameters of the atoms to which they were bonded (1.5 \times for methyl, 1.2 \times for others). Calculations used

Table 1. Summary of crystal data.

	(^t Hap) ₃ Mo · C ₆ H ₆	(^t Bu ₂ ap) ₃ Mo · CDCl ₃ · 2.5 CH ₃ CN	(^{CH3O} ap) ₃ Mo · 0.67 CH ₃ CN	(^{CF3} ap) ₃ Mo · 2.5 CHCl ₃ · CH ₃ CN	^{CF3} iq
Molecular formula	C ₆₆ H ₈₁ MoN ₃ O ₃	C ₉₀ H _{130.50} Cl ₃ DMoN _{5.50} O ₃	C _{64.33} H ₈₃ MoN _{3.67} O ₆	C _{67.50} H _{77.50} Cl _{7.50} F ₉ MoN ₄ O ₃	C ₂₁ H ₂₄ NOF ₃
Formula weight	1060.27	1541.80	1099.61	1525.65	363.41
<i>T</i> /K	120(2)	120(2)	120(2)	120(2)	120(2)
Crystal system	Monoclinic	Monoclinic	Monoclinic	Triclinic	Monoclinic
Space group	<i>P</i> 2 ₁ / <i>c</i>	<i>P</i> 2 ₁ / <i>n</i>	<i>P</i> 2 ₁ / <i>c</i>	<i>P</i> $\bar{1}$	<i>P</i> 2 ₁ / <i>c</i>
λ /Å	0.71073 (Mo K α)	0.71073 (Mo K α)	0.71073 (Mo K α)	0.71073 (Mo K α)	0.71073 (Mo K α)
Total data collected	101828	177017	372155	103484	32290
No. of indep reflns.	14696	22286	46482	18038	4710
<i>R</i> _{int}	0.0291	0.0327	0.0446	0.0693	0.0259
Obsd refls [<i>I</i> > 2 σ (<i>I</i>)]	11575	18567	37003	13295	3950
<i>a</i> /Å	15.6829(11)	13.9143(6)	28.0584(18)	14.1451(7)	10.6486(9)
<i>b</i> /Å	17.7027(13)	25.9480(12)	35.1630(18)	15.0385(10)	10.2739(5)
<i>c</i> /Å	21.1930(15)	24.7282(12)	19.4064(10)	20.0036(9)	17.2886(8)
α /°	90	90	90	94.129(2)	90
β /°	94.044(3)	93.1909(16)	106.4113(17)	100.295(2)	96.788(2)
γ /°	90	90	90	117.9600(10)	90
<i>V</i> /Å ³	5869.2(7)	8914.2(7)	18366.6(18)	3638.1(3)	1878.2(2)
<i>Z</i>	4	4	12	2	4
μ /mm ⁻¹	0.270	0.285	0.265	0.525	0.099
Crystal size/mm	0.56 × 0.26 × 0.11	0.62 × 0.37 × 0.26	0.52 × 0.34 × 0.27	0.29 × 0.26 × 0.18	0.47 × 0.34 × 0.16
No. refined params	982	1391	2074	851	331
<i>R</i> 1, <i>wR</i> 2 [<i>I</i> > 2 σ (<i>I</i>)]	<i>R</i> 1 = 0.0337 <i>wR</i> 2 = 0.0798	<i>R</i> 1 = 0.0339 <i>wR</i> 2 = 0.0865	<i>R</i> 1 = 0.0399 <i>wR</i> 2 = 0.0906	<i>R</i> 1 = 0.0581 <i>wR</i> 2 = 0.1475	<i>R</i> 1 = 0.0369 <i>wR</i> 2 = 0.0965
<i>R</i> 1, <i>wR</i> 2 [all data]	<i>R</i> 1 = 0.0532 <i>wR</i> 2 = 0.0901	<i>R</i> 1 = 0.0445 <i>wR</i> 2 = 0.0920	<i>R</i> 1 = 0.0584 <i>wR</i> 2 = 0.0989	<i>R</i> 1 = 0.0909 <i>wR</i> 2 = 0.1655	<i>R</i> 1 = 0.0453 <i>wR</i> 2 = 0.1013
Goodness of fit	1.033	1.031	1.077	1.042	1.041

SHELXTL (Bruker AXS),¹³ with scattering factors and anomalous dispersion terms taken from the literature.¹⁴ Further details about the structures are in Table 1.

Variable-Temperature NMR Spectroscopy

Variable-temperature NMR spectra were acquired in toluene-*d*₈ and lineshapes were simulated using *i*NMR.¹⁵ To measure the rate of C-N bond rotation, the two *ortho* hydrogen resonances (δ 4–6 ppm) were simulated, while the trigonal twisting rate was measured by simulating the *tert*-butyl peaks of the *fac* and *mer* isomers. For temperatures above the coalescence point, chemical shifts of the two resonances were estimated by linear extrapolation of the temperature-dependent shifts, and the extrapolated difference in chemical shift was treated as fixed in the simulation.

Computational methods

Geometry optimizations were performed on *fac*-(^tHap)₃Mo using density functional theory (B3LYP, SDD basis set for molybdenum and a 6-31G* basis set for all other atoms), using the Gaussian09 suite of programs.¹⁶ The initial structure used was the X-ray structure of *fac*-(^tHap)₃Mo, with all *tert*-butyl groups replaced by hydrogen. No symmetry constraints were applied during the

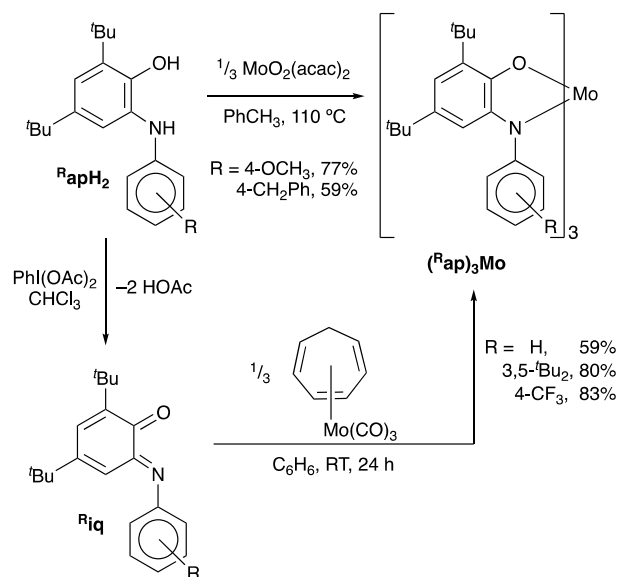
calculation, but the structure optimized to a C₃-symmetric minimum with only trifling deviations from idealized symmetry. The optimized geometries were confirmed as minima by calculation of vibrational frequencies. Plots of calculated Kohn-Sham orbitals were generated using Gaussview (v. 5.0.8) with an isovalue of 0.04.

Results

Synthesis and structure of tris(amidophenoxide)molybdenum(VI) complexes

The preparation of catecholate or amidophenoxide complexes of molybdenum or tungsten typically involves reacting the reduced ligand species (catechol or aminophenol) with a hexavalent metal source such as dioxobis(acetylacetonato)molybdenum(VI)^{6,17,18} or tungsten hexachloride.¹⁹ Indeed, prolonged heating of a variety of substituted *N*-aryl-4,6-di-*tert*-butyl-2-aminophenols (^RapH₂) with MoO₂(acac)₂ in toluene at 110 °C produces the corresponding tris(amidophenoxide) complexes (^Rap)₃Mo (Scheme 1), which can be isolated after crystallization from acetonitrile.

This method is not always convenient, due to the long reaction times and the difficulty of achieving complete reaction, as the products are sensitive to water and will slowly react at room temperature with the water released as a byproduct of the reactions to give hydrolysis products (see Figures S1-S2 in the ESI). An alternative strategy for preparing group 6 catecholates complexes is reaction of $\text{Mo}(\text{CO})_6$ ²⁰ or $\text{W}(\text{CO})_6$ ²¹ precursors with *o*-benzoquinones. The analogous reaction of an *N*-aryliminobenzoquinone would have the advantage of avoiding water as a byproduct, and would likely be relatively rapid,



Scheme 1. Preparation of iminoquinones and $(\text{R}^{\text{ap}})_3\text{Mo}$ complexes.

particularly if a more reactive $\text{Mo}(0)$ precursor such as (cycloheptatriene) $\text{Mo}(\text{CO})_3$ were used.³ Sterically unhindered *N*-aryliminoquinones have not been reported as pure compounds, but have been generated by lead tetraacetate oxidation of the corresponding aminophenols.²² The *N*-*tert*-butyliminoquinone has been prepared by PhICl_2 oxidation of the dilithiated aminophenol,²³ while 2,6-disubstituted *N*-aryliminoquinones are generally prepared by acid-catalyzed condensation of the corresponding aniline with 3,5-di-*tert*-butyl-1,2-benzoquinone.²⁴ We find that *N*-arylimino-1,2-benzoquinones are conveniently generated by treatment of the corresponding arylaminophenols with one equivalent of iodobenzene diacetate in chloroform solution at room temperature. Reaction times vary from ten minutes (for unsubstituted or alkyl-substituted compounds) to a day (for the *p*-trifluoromethylphenyl derivative), and the reaction fails for the *p*-methoxyphenyl derivative, which reacts to give uncharacterized products. After evaporation of the volatiles, the crude iminoquinones are sufficiently pure to be used in preparations of the molybdenum complexes, but they may be freed from traces of iodobenzene and acetic acid by crystallization from pentane at -30 °C. They are stable

indefinitely in the solid state under nitrogen at -30 °C, but decompose in solution over a week at room temperature. NMR spectra show predominantly the *E* isomer, but traces of the *Z* isomer are also present, as has been observed in other 1,2-iminobenzoquinones.²⁴ Reaction of cycloheptatrienemolybdenum tricarbonyl with three equivalents of iminobenzoquinone proceeds smoothly over the course of 24 h at room temperature to give $(\text{R}^{\text{ap}})_3\text{Mo}$ in good yield (Scheme 1).

The structure of the *p*-trifluoromethylphenyl iminobenzoquinone CF_3iq has been determined in the solid state (Figure 1), and shows short C-O and C-N bonds and C-C bond alternation in the six-membered ring (Table 2), as expected for an iminoquinone and observed in the *N*-*t*Bu²³ and

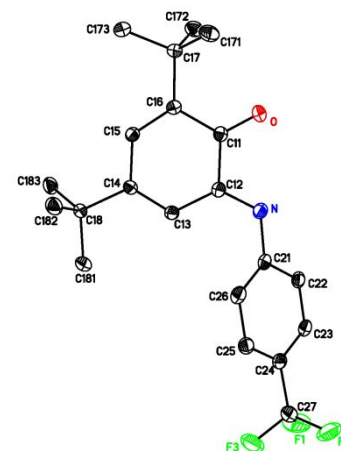


Figure 1. Thermal ellipsoid plot of CF_3iq , with hydrogen atoms omitted for clarity.

N-2,6-*i*Pr₂C₆H₃²⁵ derivatives. The slight twisting of the six-membered ring out of planarity (O–C11–C12–N dihedral angle of 15.9°) is also typical of 1,2-(imino)benzoquinones and may be due to minimizing repulsions between the heteroatom lone pairs or due to minimizing the antiaromaticity of the nominally 4π electron system in the six-membered ring.

Four of the tris(amidophenoxide) complexes have been structurally characterized by X-ray diffraction. Most strikingly, the solid state structures all show *fac* coordination about the molybdenum center (Figure 2 and Figures S3-S5). This result contrasts with all other unconstrained transition metal tris(iminoxolene) complexes, which universally have the *mer* configuration.²⁶ Known lanthanide tris(iminosemiquinones) are also *mer*,²⁷ but the tris chelate of tin with the 2,6-diisopropylphenyl ligand is *fac* in the solid state.²⁸ A *fac* geometry is only observed for transition metals in complexes of the tris(amidophenoxide) ligand MeClamp,^{6,29} where the

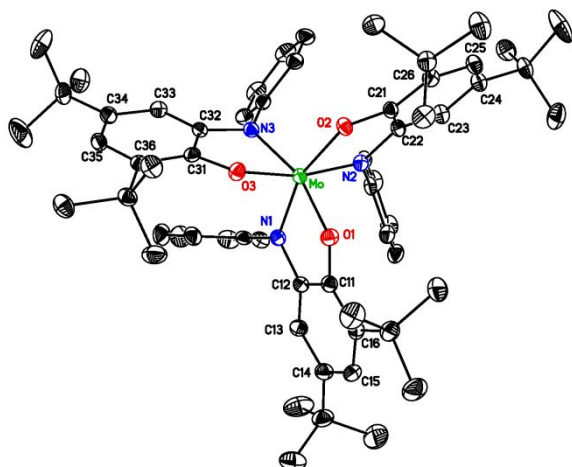


Figure 2. Thermal ellipsoid plot of $(^{\text{H}}\text{ap})_3\text{Mo}$. Hydrogen atoms have been omitted for clarity.

central tri-*p*-tolylamine core enforces it, and dimetallic complexes L_3M_2 of a 1,3-phenylenediamine-bridged bis(iminoxolene), where the binding of the ligand to a second metal serves as a similar *fac*-enforcing constraint.^{11,30} Presumably the normal predisposition toward a *mer* geometry is due to its lower steric congestion. In *fac*- $(^{\text{H}}\text{ap})_3\text{Mo}$, for example, each phenyl ring is held very close to the adjacent phenyl group, with the closest *ortho* hydrogen approaching the adjoining ring centroid at a distance of 2.63(3) Å. The four structures are all essentially identical (Table 2). In particular, analysis of the intraligand distances using established correlations³¹ gives a value for the metrical oxidation state (MOS) of -1.64 , within experimental error, for all the compounds regardless of aryl group substituent. The value

Table 2. Metrical data for structurally characterized compounds.

	$(^{\text{H}}\text{ap})_3\text{Mo} \cdot \text{C}_6\text{H}_6$ X-ray	$(^{\text{H}}\text{ap})_3\text{Mo}$ DFT	$(^{\text{tBu}^2}\text{ap})_3\text{Mo} \cdot$ $\text{CDCl}_3 \cdot 2.5 \text{CH}_3\text{CN}$	$(^{\text{CH}_3\text{O}}\text{ap})_3\text{Mo} \cdot 2$ CH_3CN	$(^{\text{CF}_3}\text{ap})_3\text{Mo} \cdot 2.5$ $\text{CHCl}_3 \cdot \text{CH}_3\text{CN}$	CF_3iq
<i>Bond distances / Å</i>						
Mo–O1	1.995(12)	2.021	2.000(7)	1.993(9)	1.995(5)	
Mo–N1	2.007(7)	2.039	2.002(4)	2.007(8)	2.015(3)	
O1–C11	1.330(3)	1.327	1.327(2)	1.327(4)	1.333(5)	1.2143(13)
N1–C12	1.393(2)	1.398	1.397(2)	1.395(4)	1.392(6)	1.2857(13)
C11–C12	1.403(2)	1.421	1.403(3)	1.404(4)	1.410(5)	1.5236(14)
C12–C13	1.396(2)	1.405	1.400(4)	1.397(4)	1.393(9)	1.4495(14)
C13–C14	1.376(2)	1.393	1.383(6)	1.381(6)	1.380(5)	1.3445(14)
C14–C15	1.403(3)	1.404	1.400(7)	1.405(7)	1.406(9)	1.4662(14)
C15–C16	1.387(3)	1.394	1.387(4)	1.386(4)	1.388(6)	1.3471(14)
C11–C16	1.402(2)	1.400	1.404(3)	1.402(5)	1.402(5)	1.4803(14)
Metrical Oxidation State (MOS) ³¹	–1.69(12)	–1.63(10)	–1.64(10)	–1.62(10)	–1.62(7)	+0.23(10)
<i>Bond angles / °</i>						
O1–Mo–N1	77.1(5)	76.7	77.0(2)	77.0(4)	77.0(14)	
O1–Mo–N3	100(3)	99.3	99.8(8)	101(3)	101(2)	
O1–Mo–O2	90(3)	90.3	88(2)	89(2)	91(2)	
N1–Mo–N2	94(2)	95.7	97(2)	95(3)	94(2)	
N1–Mo–O3	163(3)	163.7	163(2)	162(3)	162(2)	

Bond distances and angles are reported as the average of chemically equivalent values in the crystals, with esds combining the variance of the observed values with the estimated esds from the crystallographic model. The numbering given is the lowest-numbered instance in the structure. DFT-calculated values refer to the compound with *tert*-butyl groups replaced by hydrogen.

calculated by density functional theory (DFT) methods is the same as this within experimental uncertainty. Such noninteger MOS values have been interpreted in similar compounds as indicative of significant π donation from a (formally) amidophenoxide ligand to Mo(VI). The values seen here are similar to those seen in the seven-coordinate tris(amidophenoxide) (MeClamp)Mo (MOS = $-1.47(5)$ and $-1.58(6)$ in two different crystal structures)⁶ and the bis(amidophenoxide)-mono(catecholate) complex $(^{\text{tBu}}\text{Clip})\text{Mo}(3,5\text{-}^{\text{tBu}}\text{Cat})$ (MOS = -1.66 avg).⁴

Dynamics and Isomerism

The ^1H NMR spectrum of $(^{\text{H}}\text{ap})_3$ at low temperature (Figure 3) is consistent with the presence of a single, C_3 -symmetric isomer, in which rotation about the C–N bond is slow on the NMR timescale. In particular, the two *ortho* resonances have very different chemical shifts (δ 4.75 and 6.60 in toluene- d_8 at -61 °C), with the strong upfield shift of the former resonance consistent with the positioning of one of the *ortho* hydrogens in the shielding cone of the adjacent phenyl group. This strongly suggests that the *fac* isomer found in the solid state is also observed in solution at low temperature.

As the temperature is raised, two sets of changes in the ^1H NMR spectrum of $(^{\text{H}}\text{ap})_3\text{Mo}$ become apparent. First, the *ortho*

resonances of the complex broaden and then coalesce (at about 0 °C) into a single peak, which then sharpens as the temperature is raised further. Similar changes affect the *meta*-phenyl resonances (though the coalescence temperature is much lower due to the much smaller difference in chemical shift), but all other signals remain sharp. This indicates a fluxional process that exchanges the two sides of the aryl ring. This could be occurring either through C–N bond rotation, or through a trigonal Bailar twist that would go through a transition state^{32,33} with C_{3v} symmetry. To distinguish between the two mechanisms, we examined the spectra of the compound with a *para*-benzyl substituent, $(^{PhCH_2}ap)_3Mo$. The two methylene hydrogens in this compound are diastereotopic in the C_3 -symmetric *fac* isomer and remain so regardless of the rate of C–N bond rotation, while a Bailar twist would render the two methylene hydrogens equivalent. Even at room temperature (Figure 4), where the *ortho* hydrogens are exchanging with $k = 2000\text{ s}^{-1}$, the methylene hydrogens are diastereotopic, appearing as a sharp AB quartet. The fluxional process is therefore concluded to involve C–N bond rotation, with the Bailar twist being too slow to observe by dynamic NMR. Activation parameters for C–N bond rotation for the four *para*-substituted complexes were ascertained from Eyring plots of rate constants determined by lineshape simulation (Figure 5) and are compiled in Table 3.

The second set of changes observed in the NMR spectra of $(ap)_3Mo$ as the temperature is raised is the appearance of a second set of resonances (marked with * in Figures 3–4), indicating the appearance of the *mer* isomer as a minor component in solution. The spectrum of the minor isomer appears symmetrical at all temperatures at which it is abundant enough to be observed (above –30 °C or so, depending on the aryl substituent), consistent with a rapid trigonal (Rây-Dutt) twist that interconverts the three different chelate environments of the *mer* isomer (see below).

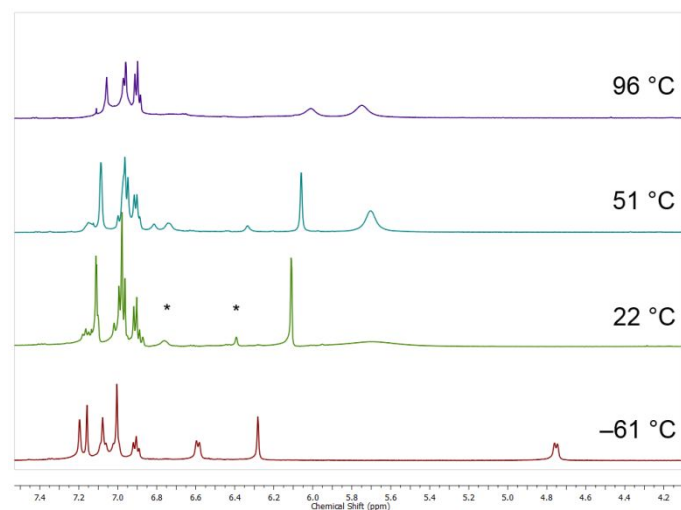


Figure 3. Variable-temperature 1H NMR spectra (aromatic region) for $(Hap)_3Mo$ (toluene- d_6 , 500 MHz). Peaks due to the *mer* isomer are marked with * in the 25 °C spectrum.

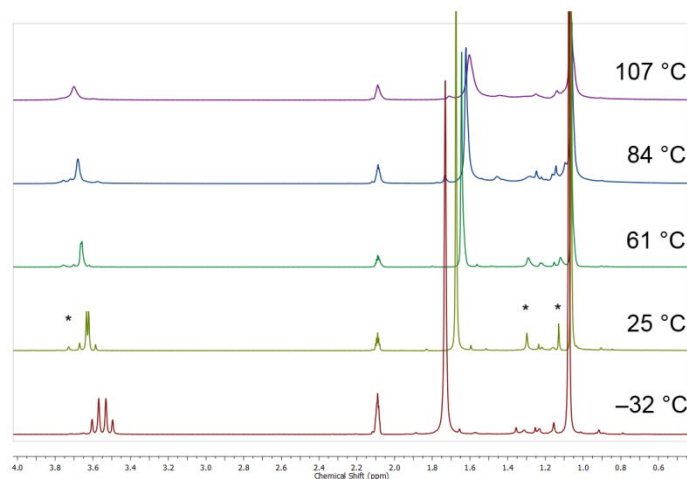


Figure 4. Variable-temperature 1H NMR spectra (aliphatic region) for $(^{PhCH_2}ap)_3Mo$ (toluene- d_6 , 400 MHz). Peaks due to the *mer* isomer are marked with * in the 25 °C spectrum.

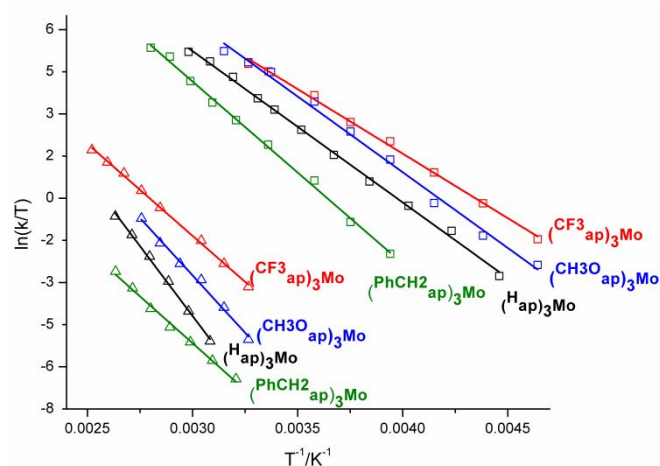


Figure 5. Eyring plot for C–N rotation (squares) and isomer interconversion (triangles).

Table 3. Activation parameters for aryl C–N bond rotation, and activation parameters and thermodynamics of *fac* → *mer* conversion, of *p*-substituted (^hap)₃Mo complexes. ΔH and ΔG values are in kcal mol⁻¹, ΔS in cal mol⁻¹ K⁻¹.

	C–N Bond Rotation			Isomerization Kinetics (<i>fac</i> → <i>mer</i>)			Isomerization Thermodynamics (<i>fac</i> → <i>mer</i>)		
	ΔH^\ddagger	ΔS^\ddagger	ΔG^\ddagger_{298}	ΔH^\ddagger	ΔS^\ddagger	ΔG^\ddagger_{298}	ΔH°	ΔS°	ΔG°_{298}
<i>p</i> -CH ₃ O	10.7(3)	-2.5(12)	11.4(3)	16.2(6)	-4.0(19)	17.4(6)	1.94(5)	3.4(2)	0.93(5)
<i>p</i> -PhCH ₂	12.9(3)	-0.3(9)	11.4(2)	13.2(4)	-18(2)	16.3(9)	3.28(8)	5.3(3)	1.69(8)
<i>p</i> -H	10.7(2)	-4.7(6)	12.1(2)	19.7(5)	3.7(14)	18.6(5)	2.37(4)	4.8(13)	0.94(4)
<i>p</i> -CF ₃	9.1(2)	-7.6(7)	13.0(3)	13.0(9)	-11(2)	18.6(4)	0.31(2)	1.09(9)	-0.01(2)

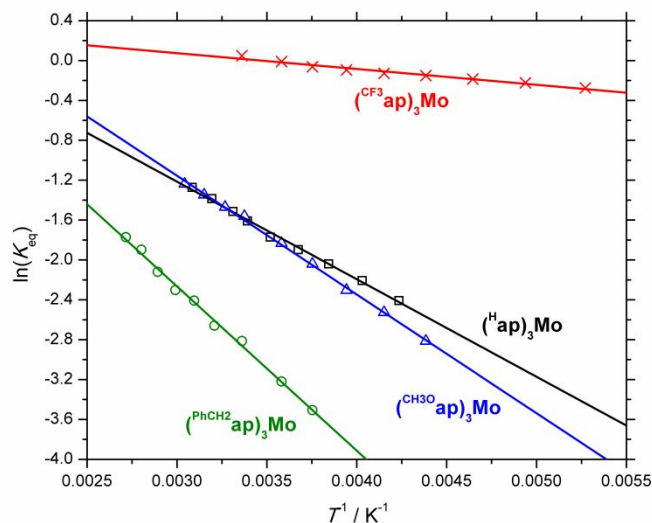


Figure 6. van't Hoff plots for *fac* → *mer* interconversion of (^hap)₃Mo.

The proportion of *mer* isomer increases with increasing temperature (Figure 6), and the resonances begin to broaden above about 50 °C (Figure 3) as the signals of the minor isomer begin to exchange with those of the major isomer. Activation parameters for the isomer interconversion (Table 3) generally show the modest negative activation entropies typical of trigonal twists.³⁴

Electronic structure of (^hap)₃Mo

In the C₃ symmetry of the tris(amidophenoxide) complex *fac*-(^hap)₃Mo, the redox-active orbitals (RAOs) of the amidophenoxides transform as *E* + *A*, as do the *dπ* orbitals of the molybdenum. The two *E* sets overlap strongly, forming a pair of π bonding and a pair of π antibonding orbitals (Figure 7). The *A*-symmetry orbitals, in contrast, overlap much more weakly. Were the ligand symmetrical—catecholates³⁵ or benzenediamide—then the two orbitals would be strictly orthogonal, with the *d*_{z²} orbital transforming as *A*₁ and the RAO combination transforming as *A*₂ in *D*₃ symmetry. Thus, any overlap between the *A*-symmetry metal and ligand orbitals must be due to the asymmetry of the ligand orbital. The nitrogen atom makes a greater contribution to the RAO than does oxygen,

and thus there is perceptible overlap, but the orbitals have much less bonding character than the *E* orbitals.

The complex shows a number of intense ($\epsilon = 1\text{--}3 \times 10^4$ L mol⁻¹ cm⁻¹) transitions in the visible spectrum (Figure 8). With the

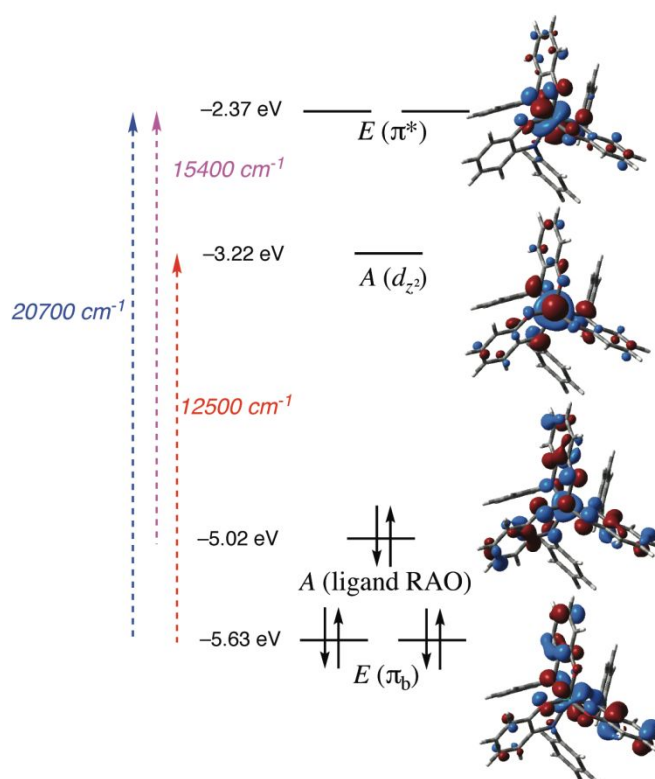


Figure 7. Molecular orbital diagram for (^hap)₃Mo. Pictures and energies are of Kohn-Sham orbitals (B3LYP, SDD/6-31G*) calculated for the compound with *tert*-butyl groups replaced with hydrogens. Frequencies are of the experimental absorption maxima (CH₂Cl₂). Only one orbital from each *E* set is shown.

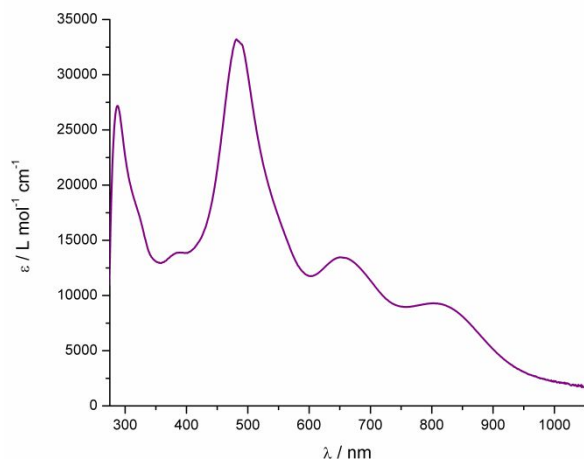


Figure 8. Optical spectrum of $(^{\text{H}}\text{ap})_3\text{Mo}$ (2.6×10^{-5} M, CH_2Cl_2).

aid of time-dependent density functional theory (TDDFT) calculations, these are assigned, in order of increasing energy, as $\pi \rightarrow d_{z^2}$ ($\lambda_{\text{max}} = 802$ nm for $(^{\text{H}}\text{ap})_3\text{Mo}$, calcd 848 nm by TDDFT), $n \rightarrow \pi^*$ (650 nm, calcd 665 nm), and $\pi \rightarrow \pi^*$ (482 nm, calcd 448 nm). (The last of these transitions encompasses a variety of bands, according to TDDFT, and experimentally a shoulder is observed on the low-energy side of the band maximum.) The HOMO–LUMO ($n \rightarrow d_{z^2}$) transition is predicted by TDDFT to occur at 1246 nm, but with zero intensity. Experimentally, the compound does not absorb between 1000 and 2000 nm.

While all the orbitals have both metal and ligand character, the filled orbitals are clearly more localized on the ligands, and the empty orbitals clearly more localized on the molybdenum. This is consistent with the structural data, where the MOS of -1.64 indicates that the compound is most reasonably described as a tris(amidophenoxide) complex of molybdenum(VI), albeit with a substantial amount of π donation from ligand to metal. Thus, the optical transitions can be described as essentially ligand-to-metal charge transfer transitions. One would thus expect electron-withdrawing *para* substituents on the ligands to lower the energy of the ligand-centered orbitals more than the metal-orbitals and thus raise the energy of the optical transitions. In fact, the reverse is true, with the most electron-poor $(^{\text{CF}_3}\text{ap})_3\text{Mo}$ showing the most red-shifted optical bands (Table 4). The *meta*-substituted $(^{\text{tBu}_2}\text{ap})_3\text{Mo}$ is anomalous, with the two lowest energy-bands extremely red-shifted, and the highest-energy band blue-shifted, compared to the other complexes. The *N*-aryl groups in these compounds are almost perpendicular to the plane of the amidophenoxide, so there is no conjugation between the substituted ring and the π system of the amidophenoxide. We therefore tentatively suggest that the unexpected effect on the optical transitions is due to the *para*-substituents acting more strongly inductively on the σ donation of the nitrogen toward the molybdenum than on the π system of the amidophenoxide. This effect is consistent with the patterns seen in the electrochemistry of the complexes (Figure 9, Table

4), where the CF_3 group shows a larger anodic shift in the (metal-centered) reduction wave than on the (ligand-centered) oxidation wave, though the difference is relatively slight.

Another trend in the substituent effects that is worthy of note is that *p*-methoxy, which would normally be expected to be the most electron-rich of the groups,³⁶ is in fact similar to H in its characteristics. This is true for all the features of the complexes: *p*-OMe is similar to *p*-H not only for the electrochemical data and the optical spectra, but also for the equilibrium and rate measurements as well. This too is consistent with a heightened impact of the inductive effects (which for OCH_3 are electron-withdrawing) over the usually dominant electron donation by resonance.

Reactivity of $(\text{ap})_3\text{Mo}$

The complex $(^{\text{H}}\text{ap})_3\text{Mo}$ hydrolyzes slowly in the presence of even small amounts of water. While the hydrolysis product

Table 4. Electrochemical data and optical transitions of iminoquinones and tris chelated molybdenum complexes $(^{\text{R}}\text{ap})_3\text{Mo}$.

Substituent	$E^\circ / \text{V vs. Fc}^+/\text{Fc}$	$\lambda_{\text{max}} / \text{nm}$
CH_3O	$-1.03, 0.10$	481, 648, 801
$^{\text{t}}\text{Bu}_2$	$-1.20, 0.18$	476, 693, 850
PhCH_2	$-1.04, 0.21$	481, 656, 816
H	$-1.00, 0.20$	482, 650, 803
CF_3	$-0.71, 0.39$	496, 678, 837

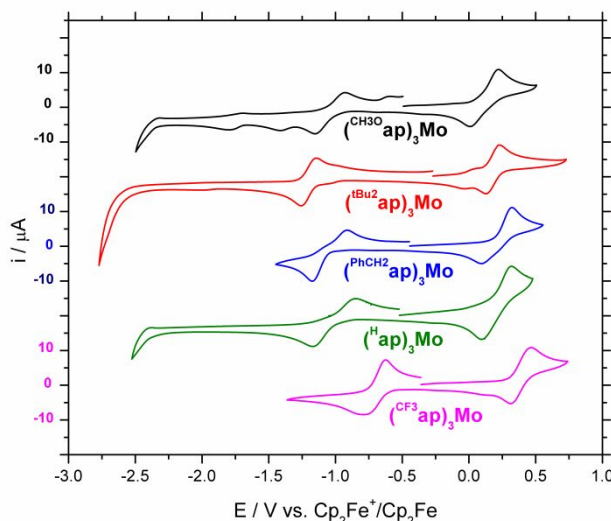


Figure 9. Cyclic voltammograms of $(^{\text{R}}\text{ap})_3\text{Mo}$ in CH_2Cl_2 (0.1 M Bu_4NPF_6 , 60 mV s^{-1}).

was not isolated, two isomers of $\{(\text{ap})(\text{apH})\text{Mo}(\text{O})_2(\mu\text{-O})\}$ ($\text{ap} = ^{\text{H}}\text{ap}$ or $^{\text{PhCH}_2}\text{ap}$), each containing an *N*-protonated ligand with the amine bonded trans to the μ -oxo ligand, were characterized crystallographically (Figures S1–S2). NMR studies show that the hydrolysis products are fluxional at room temperature, with multiple isomers interconverting (Figure S13).

The $(^H\text{ap})_3\text{Mo}$ complex does not bind Lewis bases such as pyridine or thiocyanate ion. In neat pyridine- d_5 , the NMR spectrum of $(^H\text{ap})_3\text{Mo}$ is similar to that shown in noncoordinating solvents, with signals for both *fac* and *mer* isomers observed at room temperature. This strongly suggests that no binding is observed, since the seven-coordinate species is expected to be highly fluxional³ and thus even its transient formation would catalyze isomer interconversion. The low Lewis acidity of $(^H\text{ap})_3\text{Mo}$ contrasts with the behavior of the tris(3,5-di-*tert*-butylcatecholato)molybdenum(VI) fragment, which is so electrophilic that only seven-coordinate adducts are observed,³ and of the bis(amidophenoxide)-monocatecholate complex $(^t\text{BuClip})\text{Mo}(3,5-^t\text{Bu}_2\text{Cat})$, which is isolable as a six-coordinate species but readily binds pyridine ($K_{\text{assoc}} = 500$ at 300 K).⁴ Evidently $(^H\text{ap})_3\text{Mo}$ continues the trend of decreasing electrophilicity at molybdenum as catecholates are replaced by amidophenoxides. This trend parallels the degree of π donation from the ligands, as judged by their MOS values, which become more positive in the order $(3,5-^t\text{Bu}_2\text{Cat})_3\text{Mo}(\text{py})$ (-1.77 avg)³ < $(^t\text{BuClip})\text{Mo}(3,5-^t\text{Bu}_2\text{Cat})$ (-1.72 avg)⁴ < $(^H\text{ap})_3\text{Mo}$ (-1.69), although the differences are small. The failure of seven-coordinate $(\text{MeClamp})\text{Mo}$ to react with Lewis bases was attributed to binding of the internal triarylamine nitrogen, but the present work suggests that the electronic effect of three strongly donating amidophenoxides is enough to suppress any electrophilicity at molybdenum.

Consistent with its low electrophilicity, $(^H\text{ap})_3\text{Mo}$ does not react with amine-*N*-oxides such as trimethylamine-*N*-oxide, *N*-methylmorpholine-*N*-oxide, or dimethylaniline-*N*-oxide. These nucleophilic oxidants rapidly oxidize $(^t\text{Bu}_2\text{Cat})_2\text{MoO}$ and $(^t\text{Bu}_2\text{Cat})_3\text{Mo}$ species, as well as $(^t\text{BuClip})\text{Mo}(^t\text{Bu}_2\text{Cat})$, to MoO_3 and the corresponding (imino)quinones in “nonclassical” oxygen atom transfer reactions.

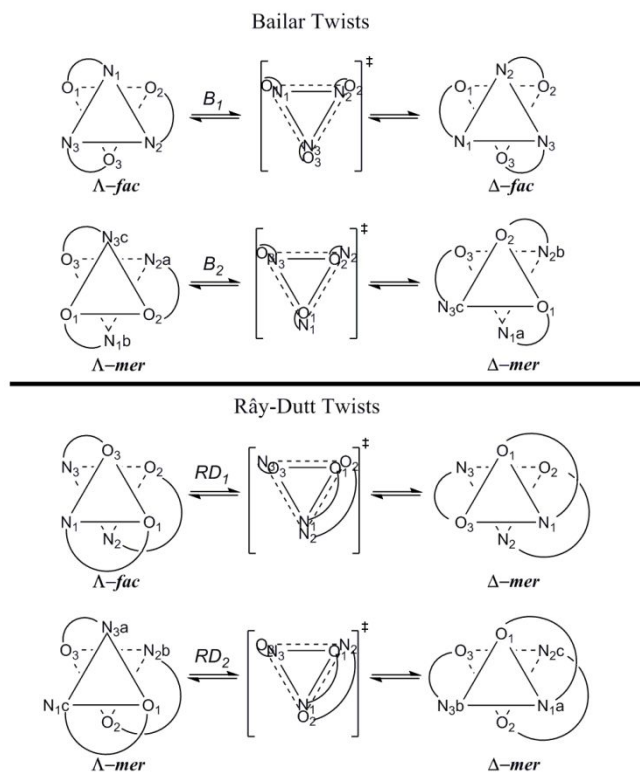
Discussion

Stereodynamics

Dynamic NMR spectroscopy indicates that the *fac* and *mer* isomers of $(\text{ap})_3\text{Mo}$ interconvert on the NMR timescale at temperatures a little above room temperature. (The low-temperature fluxional process involves C–N bond rotation and will not be discussed further.) This process presumably involves trigonal twisting, as the modest enthalpies of activation and small negative entropies of activation are not consistent with a dissociative mechanism. Facile trigonal twisting has been observed extensively in other catecholate^{2-4,34a} complexes of molybdenum. Significantly, the major *fac*- $(\text{ap})_3\text{Mo}$ isomers retain their sense of helicity at temperatures up to the point where they begin to exchange with the *mer* isomers, as judged from the diastereotopy of the methylene protons in *fac*- $(^{\text{PhCH}_2}\text{ap})_3\text{Mo}$ (Figure 4). In contrast, on the NMR timescale the *mer* isomer retains neither its helical sense, as the methylene

protons in *mer*- $(^{\text{PhCH}_2}\text{ap})_3\text{Mo}$ are not diastereotopic, nor its C_1 symmetry, as only two *tert*-butyl environments are observed. This high apparent symmetry of the *mer* isomer is observed at as low a temperature as the isomer can be observed. For the more electron-rich amidophenoxides, the equilibrium shifts so that only the *fac* isomer is observed below about -20 °C, but *mer*- $(^{\text{CF}_3}\text{ap})_3\text{Mo}$ is observed at -83 °C, and its ^tBu and CF_3 resonances in the ^1H and ^{19}F NMR spectra at this temperature are substantially broadened but not fully decoalesced.

These experimental data allow one to assess the relative rates of the four distinct (diastereomeric) trigonal twists possible for an octahedral tris(chelate) complex with an unsymmetrical ligand (Scheme 2). There are two possible Bailar twists (about the pseudo- C_3 axis) and two distinct possible R y-Dutt twists (about axes perpendicular to the pseudo- C_3 axis).³⁷ Of these four motions, only one, the R y-Dutt twist labeled RD_1 , interconverts between the *fac* and *mer* isomers. This process is therefore identified with the observed fluxional process that takes place in the 50–110 °C range. The second R y-Dutt twist, RD_2 , exchanges all of the environments of the three inequivalent ligands in a series of six successive twists of this type that cycle through all permutations of the three environments in both the Λ and Δ isomers. The Bailar twist of the *mer* isomer, B_2 , interchanges the ligands in the



Scheme 2. Possible trigonal twists for tris complexes of an unsymmetrical bidentate ligand, exemplified by an amidophenoxide. Reactions are shown so that a counterclockwise 120° rotation of the front face converts from reactant to product.

environments labeled *a* and *b* in Scheme 2, but the ligand in environment *c*, with its N trans to N and its O trans to O, remains in the *c* environment. Thus rapid twisting via B₂ alone would result in retaining four different *tert*-butyl resonances. The RD₁ exchange would render all the environments in the *mer* isomer equivalent, but would also interconvert between *mer* and *fac* isomers. Experimentally, the symmetrization of the *mer* isomer is rapid even at –83 °C while the *fac-mer* isomerization becomes perceptible only at +50 °C or so. Thus, the *mer-mer* Rây-Dutt twist RD₂ must be extremely rapid in (ap)₃Mo. (Nothing can be concluded about the rate of B₂ since it would lead to no further changes in the spectrum if RD₁ is already operating.) The Bailar twist of the *fac* isomer, B₁, would remove the diastereotopy of the methylene hydrogens in *fac*-(^{PhCH₂}ap)₃Mo. Since this is not observed until RD₁ becomes perceptible, this Bailar twist must be slower than either of the Rây-Dutt twists.

The trigonal twists in (ap)₃Mo thus increase in rate in the order B₁ < RD₁ < RD₂. This is an unusual ordering: typically, catecholate complexes undergo much faster Bailar twists than Rây-Dutt twists, presumably because the small bite-angle catecholate ligand prefers to span the compressed distances parallel to the C₃ axis.³⁸ For example, in (3,6-^tBu₂Cat)₂Mo(O)(dmsO), the Bailar twist is found to be much faster than the Rây-Dutt;^{34a} one can estimate³⁹ the difference in barriers as ~4 kcal mol⁻¹, corresponding to a rate advantage of ~10³ for the Bailar twist. Presumably the preference for RD₂ in (ap)₃Mo is due to steric effects. The *N*-aryl groups are already crowded in *fac*-(ap)₃Mo, as shown by the relatively slow rotation about the C–N bond and the strong upfield shift of one *ortho* hydrogen. In the trigonal prism with the ligands along the tetragonal edges, as in B₁ or B₂, the *cis-N*-aryl groups are even closer as the two ligands become parallel to each other rather than being canted away from each other in an octahedron. The Rây-Dutt twist RD₁ also brings two ligands (ligands 1 and 3 in Scheme 2) parallel to each other, with the *N*-aryl groups *cis* along the short tetragonal edge. Only RD₂ avoids close contacts between *N*-aryl groups on parallel ligands, since the two parallel ligands have *N*-aryl groups that point in opposite directions, and is thus sterically preferred over all the other possible twists. Since this motion remains fast at –80 °C, ΔG[‡] < 11 kcal mol⁻¹, giving it at least a ~6 kcal mol⁻¹ lower barrier than either RD₁ or B₁.

Stereochemistry and π bonding

The other stereochemical feature of note is the ground-state preference of the (ap)₃Mo compounds to adopt the *fac* configuration. This cannot be a steric effect, and indeed all other unconstrained transition metal complexes (ap)₃M (M = V, Cr, Mn, Fe, Co, Ru, Os) are known only as *mer* isomers. One tris(iminoxolene)-tin complex is observed to be *fac* in the solid state. The geometry of the tin derivative is likely driven by the *trans* influence, because the *fac* isomer allows the strongly bonded oxygen atoms (Sn–O = 2.072(3) Å) to be *trans* to the

more weakly bonded nitrogen atoms (Sn–N = 2.195(4) Å).²⁸ This is unlikely to be significant in (ap)₃Mo, given the nearly identical Mo–O and Mo–N bond distances in this compound.

Instead, we postulate that the preference for the *fac* geometry in (ap)₃Mo is driven by the slightly stronger π bonding possible in the *fac* isomer, in particular the bonding of the *A*-symmetry HOMO of the complex. Were the ligand symmetrical, like a catecholate, this orbital would be strictly ligand-localized and thus nonbonding; any bonding π overlap of one oxygen of a catecholate with the Mo *d*_{z² orbital would be canceled by unfavorable π overlap of the other oxygen. The asymmetry of the amidophenoxide ligand, with the greater density of the RAO on nitrogen compared to oxygen, allows net favorable overlap, but that overlap is substantially less in the *mer* isomer, since one ligand will be net antibonding compared to the other two. Even in the *fac* isomer, the overlap is poorer than in the *E*-symmetry orbitals, but the Mo participation is clearly appreciable, according to DFT calculations (Figure 7). This contrasts with the situation in seven-coordinate (MeClamp)Mo, where σ donation to the *d*_{z² orbital renders its participation in π bonding negligible.⁶ This is seen in the optical spectra of the two species: In (^Hap)₃Mo, the difference in energies of the π → π* and *n* → π* transitions (5300 cm⁻¹) is smaller than the corresponding difference in (MeClamp)Mo (7600 cm⁻¹).}}

The attribution of the stereochemical preference for the *fac* isomer to differences in π bonding is generally consistent with the observed substituent effects in (^Rap)₃Mo (Figure 6, Table 3). On changing the *para* substituent, the preference for the *fac* isomer increases in the order *p*-CF₃ < *p*-H < *p*-CH₂Ph, with the more strongly donating ligands showing a greater proportion of the *fac* isomer at equilibrium. The only anomaly is *p*-OCH₃, which is very similar to *p*-H, perhaps because the conformation of the *N*-aryl group, which prevents conjugation with the amidophenoxide RAO, leads to a diminution of the electron-donating resonance effects of the OCH₃ group compared to its electron-withdrawing inductive effects.

Significant π donation to the *d*_{z² is also consistent with the reactivity of (ap)₃Mo. In contrast to catecholate analogues, the compounds are not detectably Lewis acidic. Some of the low Lewis acidity may be steric in origin, since *intramolecular* donation of the weakly basic triarylamine nitrogen is observed in (MeClamp)Mo.⁶ But there is likely a sizable electronic component to the low Lewis acidity as well. While the ligands are best thought of as amidophenoxides, the significant amount of π bonding implies a partial transfer of electron density onto the molybdenum center. This creates a significant Mo contribution to the HOMO (Figure 7), which would tend to cause a repulsive interaction with an incoming ligand.}

Conclusions

Substituted tris(amidophenoxide)molybdenum complexes can be synthesized from the appropriate aminophenol and hexavalent $\text{MoO}_2(\text{acac})_2$, or from the iminoquinone and zerovalent (cycloheptatriene) $\text{Mo}(\text{CO})_3$. In the solid state, $(\text{ap})_3\text{Mo}$ complexes display a *fac* geometry, and this isomer is also the major species observed in solution. The *fac* and *mer* isomers interconvert in solution through a Rây-Dutt twist, which is (unusually) faster than Bailar twisting in this system, presumably for steric reasons. The preference for the *fac* isomer is attributed to enhanced π bonding in this isomer compared to the *mer* compound, consistent with a generally increased *fac* : *mer* ratio seen with more electron-rich amidophenoxides. The importance of π bonding in these complexes is also seen in the structural data, which show evidence of strong ligand-to-metal π donation in the intraligand bond distances; in the electronic spectroscopy, which is well described by a bonding model with significant splitting between π bonding levels; and in their reactivity, where the metal has no discernible Lewis acidity.

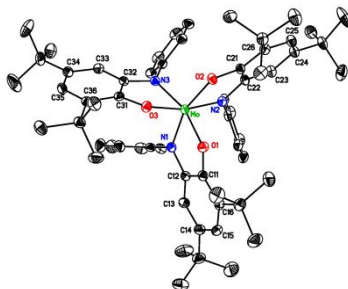
Acknowledgments

We thank Dr. Allen G. Oliver for his assistance with the X-ray crystallography. This work was supported by the US National Science Foundation (grant CHE-1465104).

Notes and references

- R. F. Munhá, R. A. Zarkesh and A. F. Heyduk, *Dalton Trans.*, 2013, **42**, 3751-3766.
- T. Marshall-Roth, S. C. Liebscher, K. Rickert, N. J. Seewald, A. G. Oliver and S. N. Brown, *Chem. Commun.* 2012, **48**, 7826-7828.
- A. H. Randolph, N. J. Seewald, K. Rickert and S. N. Brown, *Inorg. Chem.*, 2013, **52**, 12587-12598.
- S. Shekar and S. N. Brown, *Dalton Trans.*, 2014, **43**, 3601-3611.
- (a) P. Chaudhuri, M. Hess, J. Müller, K. Hildenbrand, E. Bill, T. Weyhermüller and K. Wieghardt, *J. Am. Chem. Soc.*, 1999, **121**, 9599-9610. (b) A. F. Heyduk, R. A. Zarkesh and A. I. Nguyen, *Inorg. Chem.*, 2011, **50**, 9849-9863.
- T. Marshall-Roth and S. N. Brown, *Dalton Trans.*, 2015, **44**, 677-685.
- A. J. Gordon and R. A. Ford, *The Chemist's Companion*, John Wiley and Sons: New York, 1972, p. 303.
- K. Ley and F. Lober, FRG Pat. 1 119 297, 1961.
- J. Jacquet, P. Chaumont, G. Gontard, M. Orio, H. Vezin, S. Blanchard, M. Desage-El Murr and L. Fensterbank, *Angew. Chem. Int. ed.*, 2016, **55**, 10712-10716.
- O. I. Shadyro, V. L. Sorokin, G. A. Ksendzova, G. I. Polozov, S. N. Nikolaeva, N. I. Pavlova, O. V. Savinova and E. I. Boreko, *Pharm. Chem. J.*, 2003, **37**, 399-401.
- S. Mukherjee, T. Weyhermüller, E. Bothe, K. Wieghardt and P. Chaudhuri, *Dalton Trans.*, 2004, 3842-3853.
- D. Lionetti, A. J. Medvecz, V. Ugrinova, M. Quiroz-Guzman, B. C. Noll and S. N. Brown, *Inorg. Chem.*, 2010, **49**, 4687-4697.
- G. M. Sheldrick, *Acta Cryst. A*, 2008, **A64**, 112-122.
- International Tables for Crystallography*; Kluwer Academic Publishers: Dordrecht, The Netherlands, 1992, Vol C.
- iNMR (<http://www.inmr.net>)
- M. J. Frisch, G. W. Trucks, H. B. Schlegel, G. E. Scuseria, M. A. Robb, J. R. Cheeseman, G. Scalmani, V. Barone, B. Mennucci, G. A. Petersson, H. Nakatsuji, M. Caricato, X. Li, H. P. Hratchian, A. F. Izmaylov, J. Bloino, G. Zheng, J. L. Sonnenberg, M. Hada, M. Ehara, K. Toyota, R. Fukuda, J. Hasegawa, M. Ishida, T. Nakajima, Y. Honda, O. Kitao, H. Nakai, T. Vreven, J. A. Montgomery, Jr., J. E. Peralta, F. Ogliaro, M. Bearpark, J. J. Heyd, E. Brothers, K. N. Kudin, V. N. Staroverov, R. Kobayashi, J. Normand, K. Raghavachari, A. Rendell, J. C. Burant, S. S. Iyengar, J. Tomasi, M. Cossi, N. Rega, J. M. Millam, M. Klene, J. E. Knox, J. B. Cross, V. Bakken, C. Adamo, J. Jaramillo, R. Gomperts, R. E. Stratmann, O. Yazyev, A. J. Austin, R. Cammi, C. Pomelli, J. W. Ochterski, R. L. Martin, K. Morokuma, V. G. Zakrzewski, G. A. Voth, P. Salvador, J. J. Dannenberg, S. Dapprich, A. D. Daniels, O. Farkas, J. B. Foresman, J. V. Ortiz, J. Cioslowski and D. J. Fox, *Gaussian 09, Revision A.02*, Gaussian, Inc., Wallingford CT, 2009.
- J. A. Kopec, S. Shekar and S. N. Brown, *Inorg. Chem.*, 2012, **51**, 1239-1250.
- M. M. Hänninen, P. Paturi, H. M. Tuononen, R. Sillanpää and A. Lehtonen, *Inorg. Chem.*, 2013, **52**, 5714-5721.
- (a) S. M. Beshouri and I. P. Rothwell, *Inorg. Chem.*, 1986, **25**, 1962-1964. (b) D. W. Shaffer, G. Szigethy, J. W. Ziller and A. F. Heyduk, *Inorg. Chem.*, 2013, **52**, 2110-2118. (c) C. Persson and C. Andersson, *Polyhedron*, 1993, **12**, 2569-2575.
- (a) L. A. deLearie and C. G. Pierpont, *Inorg. Chem.*, 1988, **27**, 3842-3845. (b) L. G. Ranis, K. Werellapatha, N. J. Pietrini, B. A. Bunker and S. N. Brown, *Inorg. Chem.*, 2014, **53**, 10203-10216. (c) C. G. Pierpont and R. M. Buchanan, *J. Am. Chem. Soc.*, 1975, **97**, 4912-4917. (d) M. E. Cass and C. G. Pierpont, *Inorg. Chem.*, 1986, **25**, 123-125. (e) L. Calucci, G. Pampaloni, C. Pinzino, and A. Prescimone, *Inorg. Chim. Acta*, 2006, **359**, 3911-3920.
- (a) C. G. Pierpont and H. H. Downs, *J. Am. Chem. Soc.*, 1975, **97**, 2123-2127. (b) D. J. Darensbourg, K. K. Klausmeyer and J. H. Reibenspies, *Inorg. Chem.*, 1996, **35**, 1529-1534.
- P. Chaudhuri, C. N. Verani, E. Bill, E. Bothe, T. Weyhermüller and K. Wieghardt, *J. Am. Chem. Soc.*, 2001, **123**, 2213-2223.
- S. M. Carter, A. Sia, M. J. Shaw and A. F. Heyduk, *J. Am. Chem. Soc.*, 2008, **130**, 5838-5839.
- (a) G. A. Abakumov, N. O. Druzhkov, Y. A. Kurskii and A. S. Shavyrin, *Russ. Chem. Bull., Int. Ed.*, 2003, **52**, 712-717. (b) G. A. Abakumov, N. O. Druzhkov, Y. A. Kurskii, L. G. Abakumova, A. S. Shavyrin, G. K. Fukin, A. I. Poddel'skii, V. K. Cherkasov and L. S. Okhlopkova, *Russ. Chem. Bull., Int. Ed.*, 2005, **54**, 2571-2577.
- G. A. Abakumov, V. K. Cherkasov, A. V. Piskunov, I. N. Meshcheryakova, A. V. Maleeva, A. I. Poddel'skii and G. K. Fukin, *Dokl. Chem.*, 2009, **427**, 168-171.
- (a) H. Chun, C. N. Verani, P. Chaudhuri, E. Bothe, E. Bill, T. Weyhermüller and K. Wieghardt, *Inorg. Chem.*, 2001, **40**, 4157-4166. (b) Fe: S. Mukherjee, T. Weyhermüller, E. Bill, K. Wieghardt and P. Chaudhuri, *Inorg. Chem.*, 2005, **44**, 7099-7108. (c) D. Das, A. K. Das, B. Sarkar, T. K. Mondal, S. M. Mobin, J. Fiedler, S. Záliš, F. A. Urbanos, R. Jiménez-Aparicio, W. Kaim and G. K. Lahiri, *Inorg. Chem.*, 2009, **48**, 11853-11864. (d) A. K. Das, R. Hübner, B. Sarkar, J. Fiedler, S. Záliš, G. K. Lahiri and W. Kaim, *Dalton Trans.*, 2012, **41**, 8913-8921.
- M. N. Bochkarev, A. A. Fagin, N. O. Druzhkov, V. K. Cherkasov, M. A. Katkova, G. K. Fukin and Y. A. Kurskii, *J. Organomet. Chem.*, 2010, **695**, 2774-2780.

- 28 A. V. Piskunov, I. N. Mescheryakova, G. K. Fukin, A. S. Bogomyakov, G. V. Romanenko, V. K. Cherkasov and G. A. Abakumov, *Heteroatom Chem.*, 2009, **20**, 332-340.
- 29 T. Marshall-Roth, K. Yao, J. A. Parkhill and S. N. Brown, *Inorg. Chem.*, submitted.
- 30 S. Mukherjee, E. Rentschler, T. Weyhermüller, K. Wieghardt and P. Chaudhuri, *Chem. Commun.*, 2003, 1828-1829.
- 31 S. N. Brown, *Inorg. Chem.*, 2012, **51**, 1251-1260.
- 32 K. C. Fortner, J. P. Bigi and S. N. Brown, *Inorg. Chem.*, 2005, **44**, 2803-2814.
- 33 M. Amati and F. Leij, *Theor. Chem. Accts.*, 2008, **120**, 447-457.
- 34 (a) C. M. Liu, E. Nordlander, D. Schmeh, R. Shoemaker and C. G. Pierpont, *Inorg. Chem.*, 2004, **43**, 2114-2124. (b) B. J. Brisdon, G. F. Griffin, *J. Chem. Soc., Dalton Trans.*, 1975, **20**, 1999-2002. (c) B. J. Brisdon, A. A. Woolf, *J. Chem. Soc., Dalton Trans.*, 1978, **4**, 291-295. (d) K. H. Yih and G. H. Lee *J. Organomet. Chem.*, 2008, **693**, 3303-3311. (e) K. H. Yih, G. H. Lee and Y. Wang, *J. Organomet. Chem.*, 1999, **588**, 125-133. (f) J. W. Faller, D. A. Haitko, R. D. Adams and D. F. Chodosh, *J. Am. Chem. Soc.*, 1979, **101**, 865-876. (g) G. Barrado, D. Miguel, V. Riera and S. García-Granda, *J. Organomet. Chem.*, 1995, **489**, 129-135.
- 35 T. B. Karpishin, M. S. Gebhard, E. I. Solomon and K. N. Raymond, *J. Am. Chem. Soc.*, 1991, **113**, 2977-2984.
- 36 C. Hansch, A. Leo and R. W. Taft, *Chem. Rev.*, 1991, **91**, 165-195.
- 37 (a) J. G. Gordon II and R. H. Holm, *J. Am. Chem. Soc.*, 1970, **92**, 5319-5332. (b) D. J. Berg, C. Zhou, T. Barclay, X. Fei, S. Feng, K. A. Ogilvie, R. A. Gossage, B. Twamley and M. Wood, *Can. J. Chem.*, 2005, **83**, 449-459.
- 38 A. Rodger and B. F. G. Johnson, *Inorg. Chem.*, 1988, **27**, 3061-3062.
- 39 J. W. Faller, in *Encyclopedia of Inorganic Chemistry*, R. B. King, ed., John Wiley & Sons: New York, 1994, 3914-3933.



Strong π bonding in molybdenum(VI) tris(amidophenoxides) drives a preference for the *fac* geometry and quenches the metal's Lewis acidity.